J. Cosmet. Sci., 72, 711–731 (November/December 2021)

Physicochemical Properties of Textured Hair

ROGER L. MCMULLEN, TIMOTHY GILLECE AND TYLER SCHIESS
Ashland LLC, Bridgewater, New Jersey, USA (R.L.M., T.G., T.S.)

Synopsis

In this study, we investigated differences in the various properties of textured hair as compared to straight hair. As representative hair types from both ends of the spectrum, we investigated the morphological and ultrafine structural characteristics of African and Caucasian hair. We took a profound look at African hair using field emission scanning electron microscopy (FESEM), examining the exterior of the fiber as well as its interior structure by analyzing thin cross-sections of hair. We found that it has unique morphology in both the exterior and interior of the fiber. Some key features include the fiber morphology at a point of curvature, concavity in the major axis, large distribution of melanin granules, and fibrillar structures (keratins) heavily coated with biological material (presumably lipids). We further examined the lipid characteristics of African and Caucasian hair using Fourier transform infrared imaging to map the lipid distribution within the cross-section of hair. Using dynamic vapor sorption, we observed the effect of lipid distribution in African hair and its influence on water management properties. Finally, tensile strength data (break stress, percentage extension at break, etc.) agreed with data previously published in the literature. Expanding on this theme, we monitored the fracture patterns of fibers extended to break using FESEM. Overall, African hair was found to exhibit various types of fracture patterns, especially at the point of curvature of the fiber. The structures of the broken fibrillar proteins (intermediate filaments) were significantly longer in Caucasian hair than in African hair.

INTRODUCTION

Textured hair refers to hair types that have some degree of curl, twist, wave, or coil associated with them. Hair from African descent, which is the most elliptical of all human hair types, represents one limit of the textured spectrum. Some types of Asian or Caucasian straight hair, which have more circular cross-sectional shapes, are at the other limit of the texture spectrum. Hair from various ethnicities or racial origins have unique physicochemical properties (1–5). For example, African hair has a lower radial swelling rate than Asian and Caucasian hair. In terms of mechanical (tensile) properties, it is generally found that the stress and elongation at break is lower in African hair than in Asian and Caucasian hair (6). The fracture point of the fiber in African hair during tensile measurements can occur in the twist or homogenous region of the fiber, although it more often appears in the twist region (7). African hair fibers with a larger diameter tend to have looser curl, while fibers with

Address all correspondence to Roger L. McMullen, rmcmullen@ashland.com

thinner diameters tend to have tighter curl. It has also been shown that the lipid content in African hair is greater than in other hair types (8–10).

Developing an understanding of hair curvature has challenged scientists for some time and has led to a significant amount of work in this area (11–20). A number of hypotheses have been proposed to explain hair curvature, and they involve follicle anatomy, asymmetric expression of structural keratins in the precortex, variable cortical shape, keratin filament orientation (relative to the hair growth axis), asymmetric proliferation in cells that form the inner and outer root sheaths, and dermal papilla asymmetry (21).

Examining single fibers, the intrinsic optical properties (luster) of hair obtained from various ethnic origins were determined by researchers at TRI Princeton (22). They found that African and Indian hair had the greatest luster; however, it should be noted that the degree of hair color greatly influences the outcome of such results. Also, they carried out goniophotometer measurements of single stretched fibers. Luster measurements carried out on hair in its natural state are more realistic and reflect the complexity of the hair fiber assembly and its contributions to the overall optical properties, especially in textured hair (23).

Interestingly, the amino acid composition is the same for all hair types, which has been reported in several studies (24,25). A proteomics study of South Africans of indigenous African, Indian, Caucasian, and mixed ancestry was completed and identified several different protein classes (keratins, keratin-associated proteins, histone proteins, and desmosomes) in hair. However, they were unable to find a quantitative distinction between the different proteins found in each group of subjects (26). But a genome-wide association test of people living in Latin America with mixed European, Native American, and African ancestry reported a substitution on the PRSS53 protein from the protease serine S1 family that is associated with scalp hair curvature (27). As the traditional continental boundaries of race diminish, proteomics and genomics studies are becoming more important in identifying hair traits associated with racial ancestry.

One of the principal motivations for understanding the behavior and physicochemical properties of textured hair stems from unique cosmetic treatment protocols that are used by populations with these hair types. For example, hair straightening and relaxing remain popular hair procedures to modify the overall 3D structure of hair fiber assemblies. Historically, interest in elucidating structural changes to the hair fiber associated with these treatments led to a better understanding of overall hair damage (28–32).

MATERIALS AND METHODS

Studies were carried out on dark brown European (Caucasian) and two types of African hair purchased from International Hair Importers and Products Inc. (Glendale, NY) and DeMeo Brothers, Inc. (Passaic, NJ). The European hair and one type of African hair (referred to as tightly curled African hair throughout the text) were obtained from International Hair Importers and Products Inc. We purchased another type of African hair (referred to as extremely tightly curled African hair) from DeMeo Brothers, Inc. For the analyses, many fibers were collected from a single hair tress for each hair type. While the Caucasian hair was blended, the African hair types came from one individual. Before analysis, all hair was washed with a 3% (w/w) sodium laureth sulfate:cocamidopropyl betaine (12:2) mixture.

MACROPHOTOGRAPHY OF HAIR

Photographic images of hair were obtained using an Epson Perfection V550 Photo Color Scanner (Epson Seiko, Suwa, Japan) with Epson Scan (version 3.9.1.1US) software. Images were collected in 24-bit color mode at 300 dpi. Image analysis of the photographs was carried out with ImageJ (version 1.53a) software (National Institutes of Health, Bethesda, MD). The lengths of individual hair fibers in the relaxed and fully extended states were measured to determine the curl index (*CI*) of hair.

HAIR CROSS-SECTION PREPARATION

Hair obtained from tresses was sectioned using a Leica CM3050 S (Leica Microsystems GmbH, Wetzlar, Germany) cryostat equipped with a high-profile sectioning head and Leica 818 high-profile cutting blades. Note that the cryostat blade was changed after each sample. For each sample, a 25 mm aluminum specimen disk was pre-equilibrated in dry ice (−78.5°C). A small section (1/8–1/4 in. wide × 1–2 in. long) of the ¾ in. wide tress was removed from the center of the tress length. The tip-end of the damp fiber section was then held straight and perpendicular against the platform of the disk. At the interface between the disk and tip-end of the fiber bundle, a drop of distilled water was then added. The drop instantly crystallized, hence causing the tip-end of the fiber bundle to adhere to the aluminum specimen disk. By pulling gently upward on the root end of the fibers and slowly adding water to the fiber bundle, a straight rod of ice-embedded hair was produced. Separately, each embedded sample was then mounted onto the specimen head (−30°C) of the cryostat, where the chamber temperature was equilibrated at −25°C. After conditioning for at least 1 h, 5-μm–thick sections were collected in continuous mode using a sectioning speed of 60% maximum. Hair cross-sections were air-dried on paper overnight under reduced pressure.

FIELD EMISSION SCANNING ELECTRON MICROSCOPY (FESEM) OF HAIR

The cross-sections were imaged using field emission scanning electron microscopy (FESEM) to investigate the internal morphological structure of hair and to calculate the cortical cross-sectional area ($n = 100$). Cross-sections were fixed to aluminum Pelco pin stubs using 25 mm conductive carbon tabs (Ted Pella, Redding, CA) and then coated with Au/Pd using our Leica EM ACE600 sputter coater. Finally, the hair fiber cross-sections were imaged with a Hitachi SU-5000 FESEM (Hitachi High Technologies, Schaumburg, IL) using various magnifications.

FOURIER TRANSFORM INFRARED (FTIR) IMAGING OF HAIR CROSS-SECTIONS

Fourier transform infrared (FTIR) images were obtained with a PerkinElmer Spotlight 400 FTIR imaging microscope (PerkinElmer Inc., Waltham, MA), which combines an optical microscope with an FTIR spectrometer. The system consists of a linear array of mercury-cadmium-telluride detectors coupled to a precision automated X–Y sampling stage. Background spectra were collected on sample-free areas of the CaF_2 crystal, and FTIR images were obtained at 8 cm^{-1} spectral resolution in transmittance mode at 16 scans/pixel.

Cross-sectioned hair (5 μm thickness) was used to ensure a linear transmission detector response for the entire IR spectral range. For each of the scans, the spatial resolution of each pixel was 6.25 × 6.25 μm, where each pixel provided a complete mid-IR spectrum. FTIR maps were generated with ISys software (Malvern Panalytical Ltd., Malvern, UK). The concatenated images were then baseline corrected from the base of the Amide II band to 900 cm^{-1} prior to truncation of the spectra and images (150 × 150 μm). Resulting spectra were processed with GRAMS/AI™ software (Thermo Fisher Scientific, Waltham, MA).

DYNAMIC VAPOR SORPTION (DVS) OF HAIR

Water vapor absorption curves were obtained using a TA Instruments Q5000 SA sorption analyzer (TA Instruments, New Castle, DE). All experiments were conducted at 25°C with a nitrogen gas flow of 200 mL/min. Hair was cut into 1–2 mm snippets, and 10 mg ± 0.5 was loaded into a stainless-steel mesh sample pan. The following sorption-desorption procedure was applied: (1) initial drying: 60°C and 0% relative humidity (RH) for 120 min; (2) isothermal equilibration: 25°C and 0% RH for 15 min; (3) absorption curve: fiber snippets were subjected to increasing humidity in 10% RH steps from 0% to 90% RH (720 min at each step); and (4) desorption curve: after the absorption sequence, the water vapor was progressively desorbed from the sample by lowering the humidity in 10% RH steps from 90% to 0% RH (720 min at each step).

TENSILE STRENGTH MEASUREMENTS OF HAIR

Tensile strength measurements were carried out with a system manufactured by Dia-Stron Ltd. (Andover, UK) equipped with a Tensile Tester (Type MTT690), Fiber Micrometer (Type FDAS770), and Automated Loading System (ALS1500). The entire unit is housed in an ETS Controlled Environment Chamber (Model 5533) designed and built by Electro-Tech Systems, Inc. (Glenside, PA). The fiber micrometer was a Mitutoyo Laser Scan Micrometer (Model LSM-6200) from Mitutoyo Corporation (Kawasaki, Japan).

UvWin (version 3.60, build 8) software was used to operate the tensile tester system, which was controlled by a UV 1000 Control Unit and PU 1100 Pneumatics Unit (Dia-Stron Ltd.). The following parameters were used for the tests: method type–MTT680 Extension; extension—100%, mm; rate—20 mm/min; start position—30 mm; gauge force—3 *g*; maximum force—2,000 *g*; cycles—1; cycle number—1; break detect force—5 *g*; end angle—360; slices—1; filter width—32; data interval—80 ms; proportional gain—25; integral gain—2; derivative gain—50; system offset—24,650.

Fibers were crimped prior to testing using brass crimps with a custom-designed press. The length of each fiber between the two crimps was 30 mm. Studies were carried out at 65% RH and 100% RH at room temperature (22°C). The crimped fibers were placed on a black anodized aluminum carousel, also manufactured by Dia-Stron Ltd., that contained 100 small compartments to house individual fibers. Humidity was controlled by the environmental chamber for the 65% RH tests; however, 100% RH tests were carried out by adding water to the fiber compartments of the sample cassette resulting in the fiber being submerged.

RESULTS AND DISCUSSION

The analysis of textured hair consisted of a thorough analysis by FESEM of the exterior and interior of the fibers. Examination of the interior of the fibers was made possible by a cross-sectioning technique. In addition, the lipid distribution in hair was determined by examining cross-sections of textured hair with FTIR imaging and comparing these data with those obtained for Caucasian hair. Overall, the lipid levels are relatively higher in textured hair. This led us to investigate the water management properties of textured hair with the idea that lipid composition would certainly affect water regain and subsequent loss during the drying phase of the experiment. We also investigated the tensile properties of hair, confirming that less force is required to break African hair. Examination of the fibers after break revealed that the fracture zone in the African hair cortex is distinct from Caucasian hair, while presenting a more fibrous appearance.

CHARACTERISTICS OF AFRICAN HAIR

One of the most striking characteristics of highly textured African hair is its geometrical configuration into a three-dimensional fiber assembly. Unlike straight hair, where the fibers are aligned parallel to each other, African hair has the tendency to form extremely tight curls that interweave with one another contributing to the optical properties, three-dimensional shape, and physical characteristics of the hair fiber assembly. Figure 1 contains a photograph of Caucasian straight dark brown hair and two types of African hair (tightly curled and extremely tightly curled) that were investigated in this study.

A simple way to characterize the curl of hair is to use Equation 1 to calculate the *CI*, which is obtained by dividing the length of a hair fiber in the stretched configuration to the same fiber at rest:

$$CI = \frac{Length_{stretched}}{Length_{rest}} \tag{1}$$

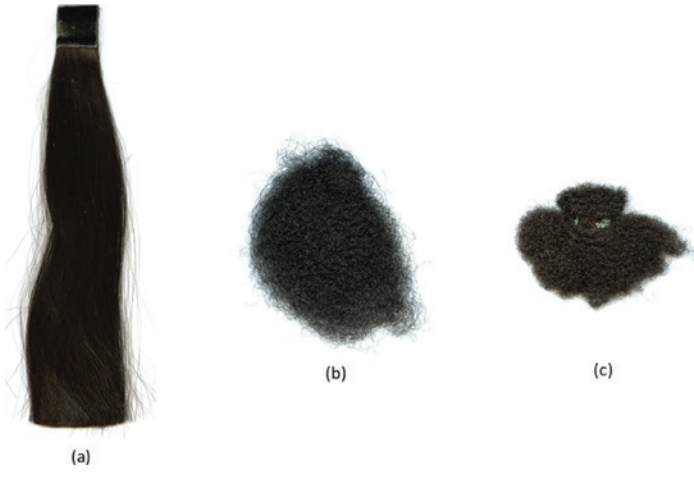

Figure 1. Hair types investigated in this study: (A) Caucasian, (B) tightly curled African, and (C) extremely tightly curled African.

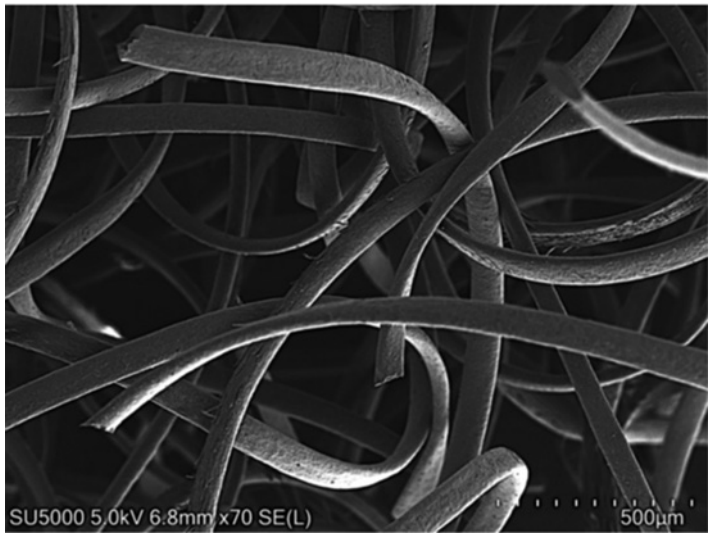

Figure 2. FESEM micrograph of a section of an African hair swatch (extremely tightly curled African hair). The cut fibers are the result of preparing a small miniature swatch from the larger swatch of hair.

The African hair types in Figure 1B (supplied by International Hair Importers and Products, Inc.) and Figure 1C (supplied by DeMeo Brothers, Inc.) were determined to have *CI* values of 0.45 ± 0.08 and 0.63 ± 0.13, respectively.

Closer examination of African hair reveals a number of interesting features that clearly distinguish it from Caucasian and Asian hair, regardless if comparing it to straight or curly hair. Figure 2 presents a FESEM micrograph of a section of an African hair tress (extremely tightly curled) where one can observe the complexity of the 3D fiber assembly. The clipped fibers in the image result from cuts made to isolate a small section of hair from the larger hair tress. Twists and turns in the fibers create a complex 3D fiber assembly where the fibers are interlaced together.

The unique morphological structure of African hair is demonstrated in the FESEM micrograph of a single hair fiber in Figure 3. Clearly, African hair has an extremely elliptical shape along the length of the fiber. Equally interesting, we find that the large face of the African hair fiber has a concave shape. In this particular hair tress, the cuticles are abraded on the small face side of the fibers. In fact, this is a common observation we have made with extremely curly African hair. Presumably, this portion of the fiber is more susceptible to grooming damage due to its inherent morphological shape. It should be noted that a minimum of 20 fibers were examined from each hair tress. The FESEM micrographs reported in this work are representative of common features found for a particular sample set.

Figure 4 presents a FESEM micrograph of another extremely tightly curled African hair fiber at its point of curvature. It can clearly be seen in the image how the fiber undergoes a twist of approximately 90° to accommodate the change in fiber orientation. Similar to the fiber shown in Figure 3, the fiber surface is also damaged, probably from repeated grooming, especially at the small face of the fiber where cuticle layers are removed. Again, note the concavity associated with the large face of the fiber.

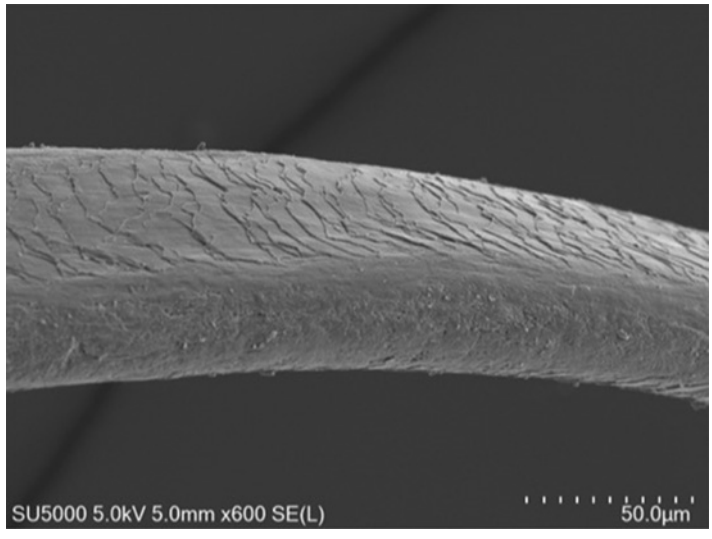

Figure 3. FESEM micrograph of extremely tightly curled African hair demonstrating its characteristic features and highly elliptical structure. Note that the root end direction of the fiber is on the right side of the image.

For comparison, Figure 5 presents a FESEM micrograph of tightly curled African hair. Again, this hair type has a *CI* value of 0.63 ± 0.13. In this particular fiber, less cuticular damage and a decreased degree of ellipticity are observed. Although we postulate that higher degrees of curliness and ellipticity could in part be responsible for the fiber's susceptibility to grooming damage, the history of the fiber is certainly a major factor in determining the extent of damage. Nevertheless, tightly curled African hair shares common features with

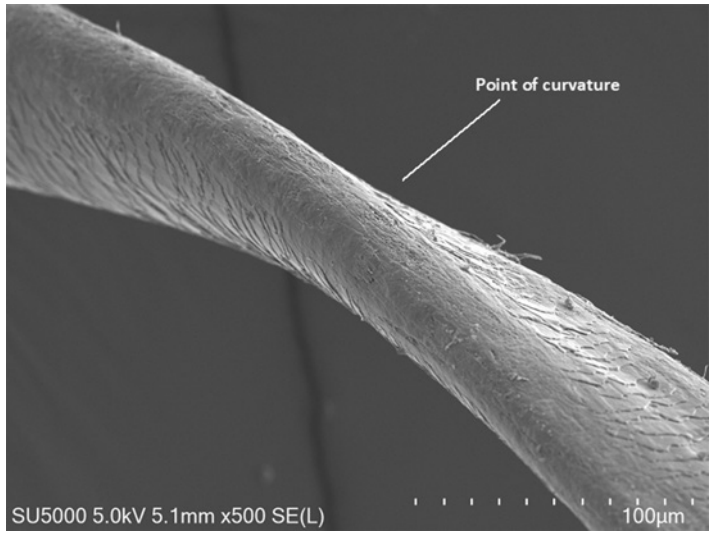

Figure 4. FESEM micrograph of extremely tightly curled African hair at one of its points of curvature. Note that the root end direction of the fiber is on the left side of the image.

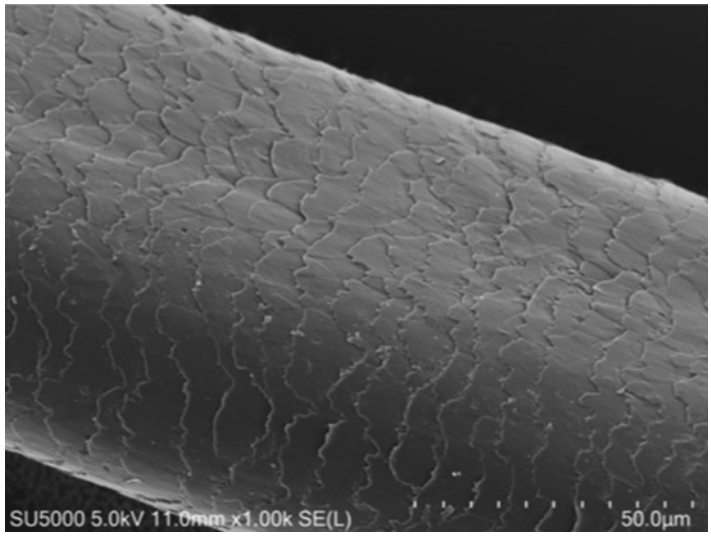

Figure 5. FESEM micrograph of tightly curled African hair. Note that the root end direction of the fiber is on the right side of the image.

extremely tightly curled African hair, however, to a lesser extent. For example, it still has a more elliptical structure than Caucasian hair and contains a certain degree of concavity along the hair axis on the large face of the fiber.

When we examine the curvature point in tightly curled African hair, we find similar behavior to that observed in extremely tightly curled African hair, as shown in Figure 6. In this case, the overall geometry appears slightly different at the curvature point, although

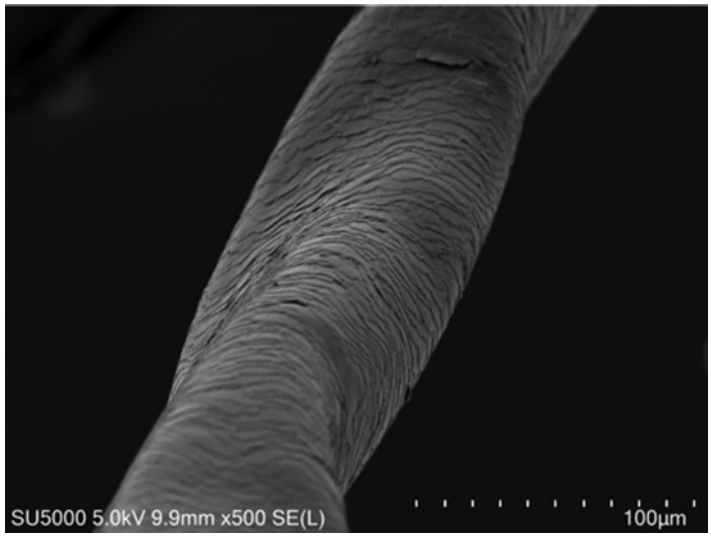

Figure 6. FESEM micrograph of tightly curled African hair at one of its points of curvature. Note that the root end direction of the fiber is at the top of the image.

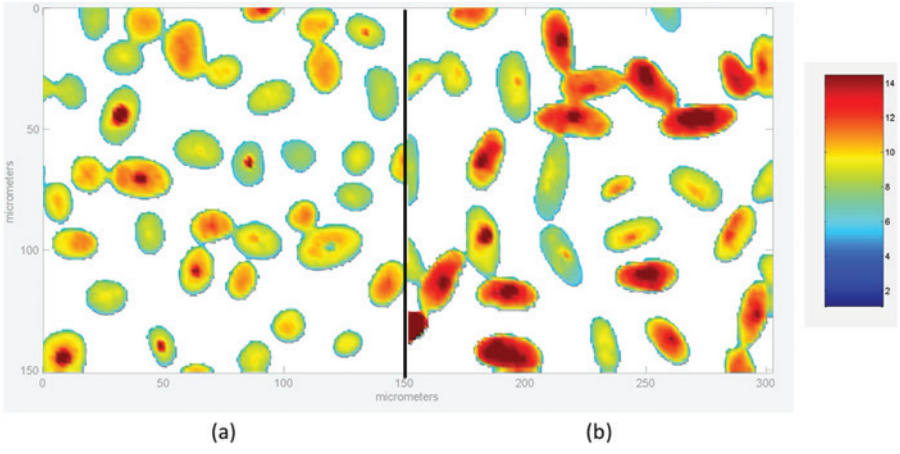

Figure 7. Spatial distribution of lipids in (A) Caucasian and (B) tightly curled African hair. Spectral images were obtained by taking the ratio of the integrated C–H symmetric and asymmetric stretching vibrations at 2,800 to 2,980 cm^{-1} to the integrated amide II band in the spectra at 1,548 cm^{-1}.

the general property of the rotation of the elliptical fiber is the same as that found in extremely tightly curled African hair.

HAIR LIPID DISTRIBUTION IN HAIR

We investigated the lipid distribution in African and Caucasian hair using FTIR imaging. Figure 7 presents FTIR images of the two hair types. In addition to the differences in shape of the cross-sections—African hair is much more elliptical than Caucasian hair—the lipid levels are greater in the African hair samples. These data were generated by normalizing the integrated intensity of the symmetric and asymmetric C–H stretch vibrations (2,800–2,980 cm^{-1}) to the peak area of the amide II frequency at 1,548 cm^{-1}. As found in previous studies, the lipid levels are relatively higher in the medulla region, followed by the cortex and then the cuticle (33,34). In Caucasian hair, the medulla region is discontinuous (as compared to Asian hair); therefore, we do not always observe a relatively distinct lipid distribution. Interestingly, almost all of the African fiber cross-sections in Figure 7 have some element of a lipid reservoir in the medulla region. Overall, our results are in agreement with previous studies that demonstrate higher levels of external lipids in African hair as compared to Asian and Caucasian hair (8–10). However, a study published by Ji et al. reported higher levels of integral lipids in Asian hair as compared to African and Caucasian hair (29).

WATER MANAGEMENT PROPERTIES OF AFRICAN VERSUS CAUCASIAN HAIR

The amount of moisture absorption and desorption by hair is often monitored to elucidate the internal structural properties of the fiber. This is typically achieved using dynamic vapor sorption (DVS), which facilitates the generation of sorption isotherms and the determination of diffusion coefficients. The amount of water in hair has a profound impact on its mechanical and material properties. Hair samples from the top, middle, and bottom of the tress were cut

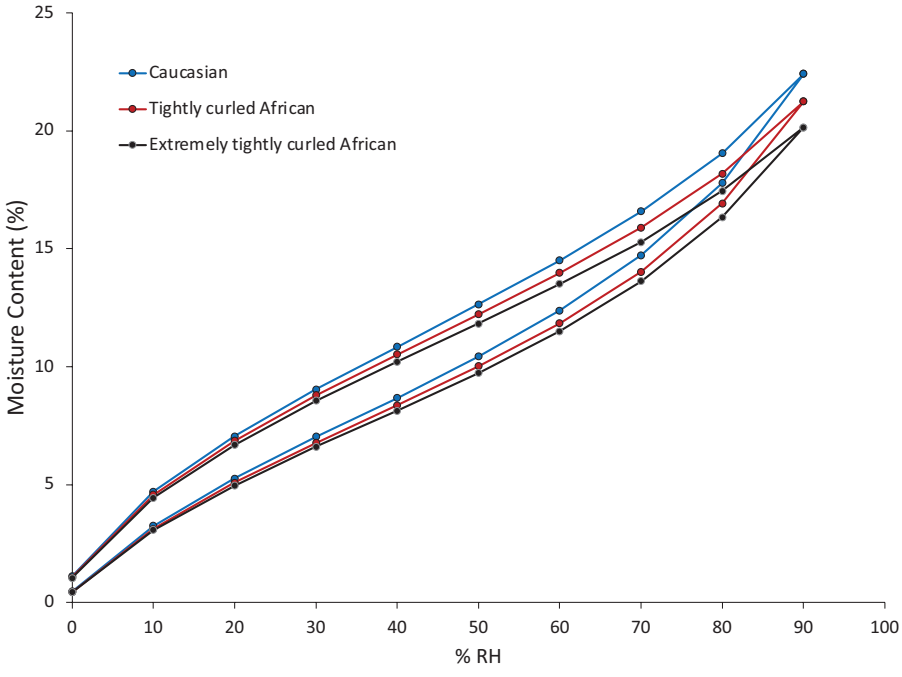

Figure 8. Hair-water absorption-desorption isotherms for (A) Caucasian, (B) tightly curled African, and (C) extremely tightly curled African hair.

into 1–2 mm snippets to probe the absorption/desorption behavior of the hair cortex. The snippets were thoroughly blended and then analyzed at 25°C. Essentially, the hair sample was placed into the DVS chamber, which contains a sensitive microbalance in a humidity- and temperature-controlled environment. Weight changes experienced by the sample are reported in terms of moisture content, which is the amount of water absorbed/desorbed per mass of hair. The samples were dried for 120 min at 60°C. The humidity was then ramped up from 0% to 90% RH at 10% RH steps (720 min at each step) to measure absorption and then ramped back down to 0% RH to monitor desorption.

There has been some controversy in the literature as to whether chemical treatments (bleaching, perming, etc.) or cosmetic treatments (e.g., a hydrophobic cationic surfactant) affect the water absorption/desorption properties of hair (35–38). Regardless, we sought to investigate if any differences could be identified between the two African hair types and Caucasian hair. Figure 8 contains isotherms for the three hair types investigated, which follow the typical sigmoidal pattern for an isotherm of hair.

The absorption and desorption isotherms for tightly curled and extremely tightly curled African hair demonstrate the lower capacity of the two African hair samples to uptake moisture as compared to Caucasian hair. At lower humidity levels, all three samples behave similarly; however, at high humidity, differences between them are more discernible. These data could suggest that the pathway for water to get into the fiber structure is more tortuous in African hair due to the greater presence of lipids. On the other hand, these differences may also be attributed to differences in protein structure. To determine if the absorption-desorption properties are influenced by protein composition, experiments on

solvent-extracted hair (to remove all lipids) for the three hair types should be carried out. The reported absorption-desorption isotherms were obtained for one tress from one lot of hair for each sample. To ensure reproducibility, we conducted the same series of tests with a second set of samples and obtained similar results.

Diffusion coefficients were calculated using Fick's second law of diffusion, which we use to describe diffusion of water vapor into (absorption) the hair fibers during a DVS experiment (39). Equation 2 is a simplified form of Fick's second law of diffusion for a cylindrical material:

$$\frac{m}{m_\infty} = 4\sqrt{\frac{Dt}{\pi r^2}} \tag{2}$$

where m is the mass at any given point in the relative humidity step, m_∞ is the mass at equilibrium (essentially when the plateau in mass change is reached), t is the time, r is the radius of the fiber, and D is the diffusion coefficient. The data obtained from the DVS experiment were plotted as $\frac{m}{m_\infty}$ as a function of $\frac{\sqrt{t}}{r}$, which allowed for the determination of the linear slope at the beginning of the plot ($\frac{m}{m_\infty} < 0.5$). The diffusion coefficient was calculated using the following relationship in units of centimeters squared per second (cm^2/s):

$$D = \frac{\pi}{16} \cdot slope^2 \tag{3}$$

Table I contains the diffusion coefficients calculated at each humidity value for absorption of water into the hair. Since Caucasian hair is oval shaped and African hair is elliptical, diffusion coefficients were calculated for the major and minor radius dimensions, and these values were averaged to obtain the diffusion coefficients reported in the table. The major and minor axes radii were obtained from FESEM measurements of hair cross-sections (at least 50

Table I
Diffusion Coefficients Determined at Each Humidity Step During DVS Absorption Experiments

% RH	African[a]	Caucasian
10	7.50×10^{-9}	2.10×10^{-8}
20	9.50×10^{-9}	2.60×10^{-8}
30	9.50×10^{-9}	2.55×10^{-8}
40	7.50×10^{-9}	2.60×10^{-8}
50	6.50×10^{-9}	2.15×10^{-8}
60	3.40×10^{-9}	1.17×10^{-8}
70	4.10×10^{-9}	1.02×10^{-8}
80	5.55×10^{-9}	1.50×10^{-8}
90	7.50×10^{-9}	2.20×10^{-8}

[a]The African hair reported is tightly curled African hair.

fibers). Overall, we find that the diffusion coefficients for Caucasian hair are greater than those obtained for African hair. Again, this could be due to the greater lipid content in African hair, which would impede the absorption of water. Notably, these diffusion coefficients are in agreement with previous studies published in the literature in the range of 10^{-8} to 10^{-9} cm^2/s (36). Please note that data are only provided for tightly curled African hair in Table I, and not extremely tightly curled African hair, because we did not carry out cross-section experiments (to measure fiber diameters with scanning electron microscopy) for this hair type.

MORPHOLOGY OF AFRICAN HAIR CROSS-SECTIONS

The highly elliptical character of African hair cross-sections has been known for some time, although detailed analyses have yet to be completed (24,40,41). In this work, we provide some insight into the morphological and fine structure of African hair. Figure 9 presents FESEM micrographs of cross-sections of Caucasian and tightly curled African hair, which clearly demonstrate the large differences in hair ellipticity between the two hair fiber types, similar to the FTIR spectral image in Figure 7. Again, extremely tightly curled African hair was not analyzed by this method due to its extraordinarily curly and kinky nature, which prevented us from carrying out the cross-sectioning procedure.

Typically, the dimensions and shape of hair along the shaft (or hair axis) are measured using a laser micrometer while rotating the fiber and examining several points along the axis of a single fiber. The advantage of this technique is that good statistics can be obtained for a selected number of fibers (usually at least 100). For comparison, we conducted measurements of the small- and large-diameter axes from the FESEM micrograph, which allowed us to calculate the cross-sectional area and ellipticity index (EI).

The cross-sectional area of Caucasian and tightly curled African hair was found to be 4,677 $\mu m^2 \pm 1{,}429$ and 6,206 $\mu m^2 \pm 1{,}223$, respectively. These data suggest that tightly curled African hair might have a slightly larger cross-section than Caucasian hair. Values in the literature of 3,857 $\mu m^2 \pm 132$ and 4,274 $\mu m^2 \pm 215$ for Caucasian and tightly curled African hair, respectively, corroborate these results (40). EI is calculated by taking the ratio of the diameter measurements of the major and minor axes. As expected, the EI of Caucasian hair (1.34 ± 0.19) was lower than tightly curled African hair (1.98 ± 0.28). Our EI data are in agreement with measurements previously reported in the literature

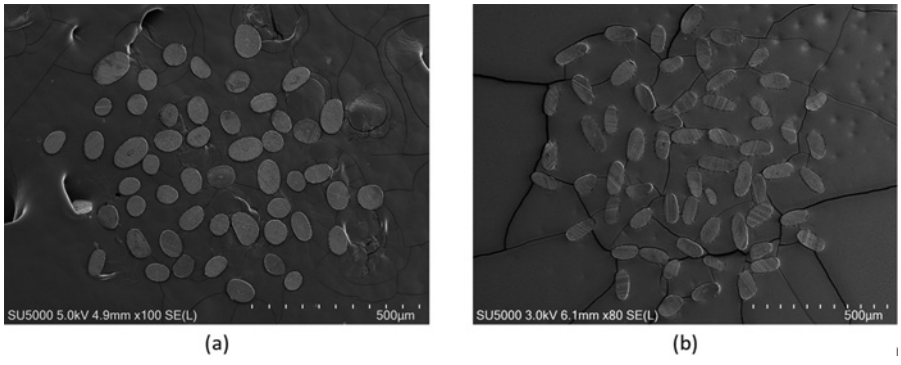

Figure 9. FESEM micrographs of cross-sections of (A) Caucasian and (B) tightly curled African hair.

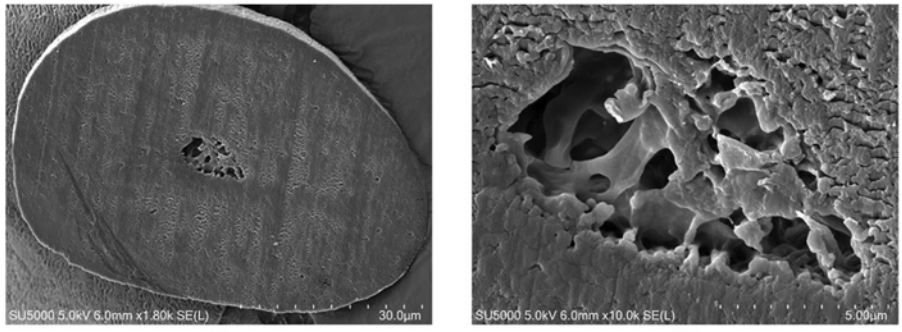

Figure 10. FESEM micrographs of a Caucasian hair fiber cross-section at magnifications of (A) ×1,800 and (B) ×10,000.

for Caucasian (1.43–1.56) and African hair (1.67–2.01) (6). It is generally accepted that the extent of curvature of human hair along its length is associated with the shape of the fiber cross-section–cylindrical versus oval versus elliptical (42,43).

One caveat to analyzing the cross-sectional shape of fibers in FESEM micrographs is the uncertainty of the hair fiber source. During the preparation procedure, the cross-sections need to be collected after each slice with the microtome to ensure that the number of measurements from each fiber is controlled. In any event, it is impossible to know the results of successive measurements on the same hair fiber using this procedure, unless, of course, cross-sections are obtained for a single fiber rather than a group of fibers.

Using FESEM, we observed many important morphological features of hair cross-sections. Figure 10A provides a FESEM micrograph of Caucasian hair where the medulla region of hair can be clearly identified in the center of the fiber. The overall cross-section is elliptical in nature, and the medulla is porous. We do not always observe the medulla in Caucasian hair as it can sometimes be discontinuous along the length of the fiber (unlike Asian cross-sections, which almost always contain a medulla). Regardless, the medulla of Caucasian hair is often characterized by its porous nature, which is illustrated by the higher-magnification image in Figure 10B.

Compared to Caucasian hair, sightings of the medulla are much less common in African hair. Figure 11 presents a FESEM micrograph of a cross-section of African hair. It appears that there is a medullary structure present close to the center of the fiber. Closer examination reveals a structure that is slightly discontinuous from the rest of the cortex. Studies have shown differences in medullary structure based on racial origin. For example, it was shown that the medulla index (ratio of medulla to overall hair fiber width) in ethnic Malays is smaller than that found in ethnic Chinese living in Malaysia (44). In a study of hair from indigenous Ghanaian individuals, it was found that the medulla could be absent, present, or discontinuous (45). The percentage occurrence of medulla for different anatomical regions decreased in the followed order: pubic, axilla, eyebrow, and scalp.

From a slightly different perspective, the growth rate of African hair (256 μm/d ± 44) was reported as significantly slower than Caucasian hair (396 μm/d ± 55) (46,47). In a study of female scalp hair, it was previously reported that the medulla of white, nonpigmented hair was more developed than pigmented hair. Surprisingly, the growth rate of nonpigmented

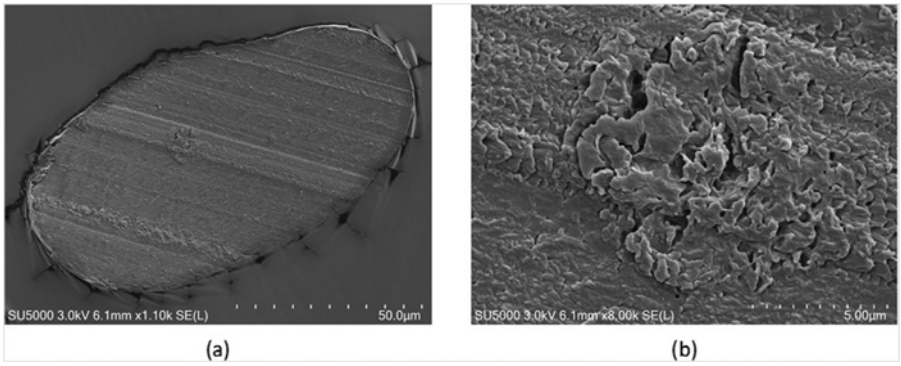

Figure 11. FESEM micrographs of an African hair fiber cross-section at magnifications of (A) ×1,100 and (B) ×8,000.

fibers (380 µm/d) was found to be greater than pigmented fibers (350 µm/d) (48). These data suggest a possible correlation between hair growth and medullary development. Furthermore, Asian hair (411 µm/d ± 53) has a faster growth rate than Caucasian or African hair and has the most developed medulla (43). Therefore, our data are in agreement with previous findings indicating that the slower growth rate of African hair leads to a more developed cortex (or less developed medulla) (49). It is also possible, but less likely, that the greater quantities of lipids (and other biological material) in the medulla of African hair make it appear less developed and porous.

We made several interesting observations related to the microtome technique that was employed. As noted in the Materials and Methods section, a stainless-steel blade was used to cut the hair cross-sections in the microtome. Ideally, use of a diamond microtome blade is preferred, as this provides extremely smooth cuts. Unfortunately, this type of blade cannot be used with all cryotomes. Therefore, researchers are often restricted to the type of blade they can employ based on the available features of their microtome. Typically, stainless-steel blades dull after the first several slices of Caucasian hair. This is clearly illustrated in Figure 12A. We found that tightly curled African hair cross-sections rarely contain such a rough cut (Figure 12B). This could suggest some fundamental structural differences

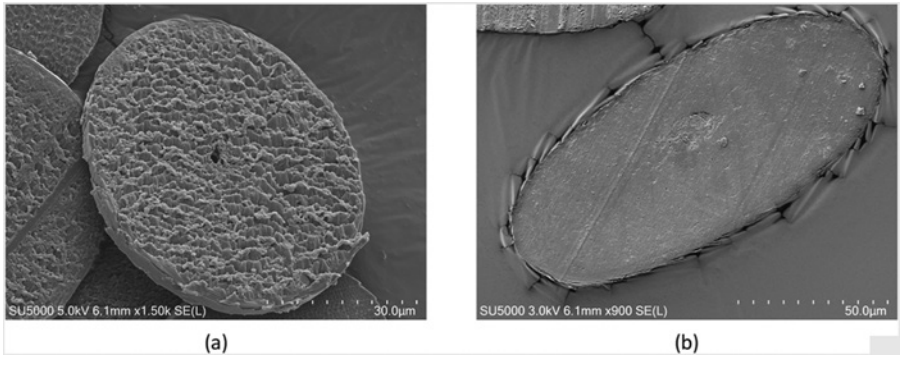

Figure 12. FESEM micrographs of (A) Caucasian and (B) tightly curled African hair demonstrating the difference in surface roughness due to the use of a stainless-steel microtome blade.

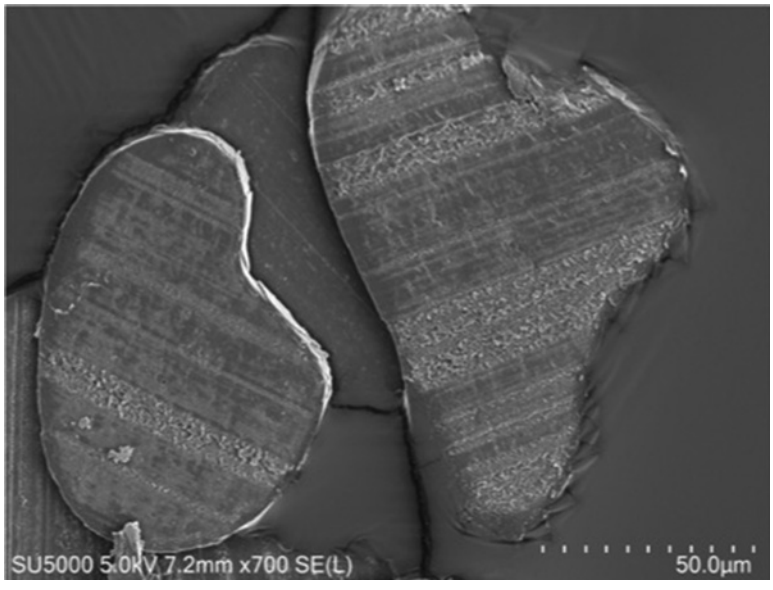

Figure 13. FESEM micrograph of diverse cross-sectional shapes of tightly curled African hair.

between the two hair types. Possibly, the greater quantity of lipids in tightly curled African hair might facilitate the cutting/slicing procedure, acting as a lubricant between the blade and the fiber. However, if tightly curled African hair had a more developed cortex, should it not be more difficult to slice?

In addition to its highly elliptical cross-sectional structure, African hair contains many other geometrical variants of its cross-sectional shape along the length of the fiber. Figure 13 presents a FESEM micrograph where two distinct shapes are represented: one that contains an oval shape with a large, rounded protrusion on its bottom right side (cross-section on the left side of the image) and another that has a more highly elliptical form with a projection on its top right side (cross-section on the right side of the image). These slices were obtained at a point of curvature along the fiber. Kamath et al. report a variety of cross-sectional shapes that are found at the curvature point of the African hair fiber (7).

At times, the microtome technique can result in fracture of the cross-sections of hair. This is nicely illustrated in Figure 14A where there are several splits within the cortex. Close examination of Figure 14A reveals a fine structural element that when imaged at higher magnification (Figure 14B) allows us to view macrofibrils grouped together. It is possible that the $3.2 \times 2.0\,\mu m$ feature in Figure 14B is a cortical cell, which is usually $5\,\mu m$ in diameter and $50\,\mu m$ in length.

Another fracture point image of tightly curled African hair is given in Figure 15. In this example, which is from the cuticle–cortex interface, we can clearly identify the macrofibrils and even melanin granules. The dimensions of the indicated macrofibrils (200 and 420 nm) fall within the generally reported range, which is about 40–500 nm (50–52). Also of interest, the indicated melanin granule in Figure 15 has the dimensions of 883×453 nm. Previous studies report melanin granule dimensions on the order of $0.3–0.6\,\mu m$ in width and $0.8–1.2\,\mu m$ in length (53). In general, we observed more melanin granules in tightly curled African as compared to Caucasian hair, although this is not a fair comparison because

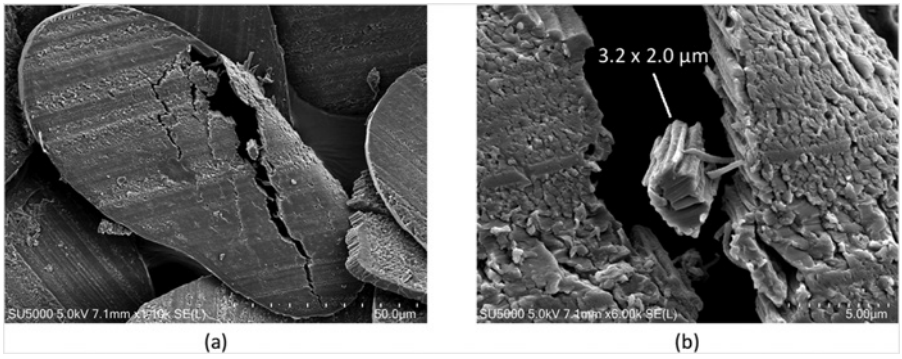

Figure 14. FESEM micrographs of tightly curled African hair showing (A) the overall fiber cross-section at ×1,100 magnification and (B) high magnification view (×6,000) at the fracture point showing one of the structural elements, which appears to contain a number of macrofibrils bound together.

we did not color match the two different hair types by a spectrophotometric technique. In this particular case, our Caucasian hair sample was European dark brown hair, which presumably should contain less melanin granules than tightly curled African hair just based on the color difference. Nevertheless, a more rigorous, quantitative study would be required to make any assumptions about the melanin content of the different hair types.

TENSILE PROPERTIES

The inherent weakness of textured hair, as compared to straight hair, has led researchers to conduct studies to better understand its mechanical properties and susceptibility to

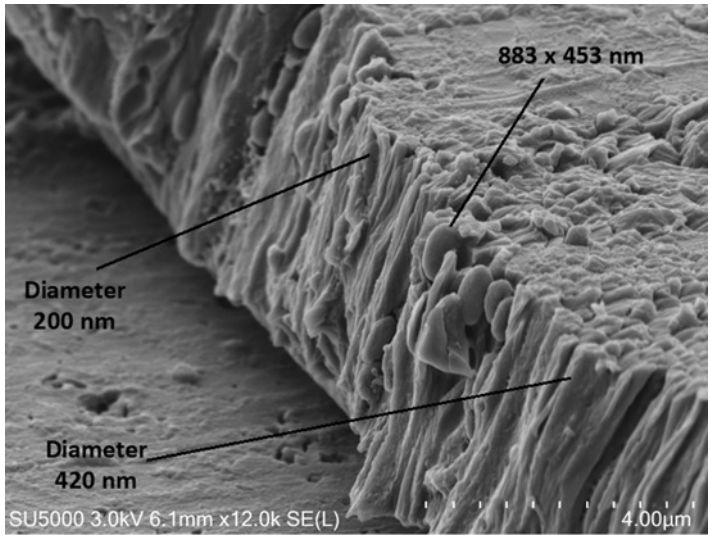

Figure 15. FESEM micrograph (×12,000 magnification) of a fractured cross-section of tightly curled African hair at the interface of the cuticle and cortex. Dimensions are provided for two of the many macrofilaments and one of the melanin granules.

Table II
Break Stress (MPa) Data for African and Caucasian Hair From This and Other Studies at Two Different Climate Conditions

Study[a]	65% RH		100% RH	
	African	Caucasian	African	Caucasian
A	191	188	156	165
B	180	178	160	155
C	148	184	94	162
D	112	180	—	—
This study	155 ± 28	194 ± 13	122 ± 23	180 ± 16

[a]The African hair reported is tightly curled African hair.
Source: Data from Studies A, B, C, and D, reported for four different locations, were published in a review article by Wolfram (6).

breakage (54–57). Tensile strength measurements of hair help us to gain insight into the mechanical strength of hair as well as the physicochemical properties of its structural components. A number of different parameters can be determined from the experimental measurements, which include Young modulus, break stress, and percentage strain at break. For demonstration, the break stresses at 65% RH and 100% RH are provided in Table II. The data obtained in this study were compared to previously published studies and found to have agreement at both climate conditions (6). Nevertheless, care should be taken when comparing tensile strength data since strain rate can affect the measured values (58). Not surprisingly, higher humidity results in lower stress break values due to water obstructing the hydrogen bonds that normally form in the matrix component of the cortex of dry hair. It should also be pointed out that African hair was found to break at lower strains.

Another aspect of tensile strength experiments is examining the hair morphology at the fracture point in the fiber. Researchers at TRI Princeton conducted a fairly comprehensive study on the fracture behavior of African hair (from one subject) in the 1980s (7). Overall, they concluded that a series of different fracture patterns could be observed in hair when it undergoes breakage in a tensile test: smooth, step, angle, fibrillate, and split end. African hair was shown to experience all types of fracture, while the predominant fracture pattern in Caucasian hair was reported as a smooth fracture. Our results indicate that African

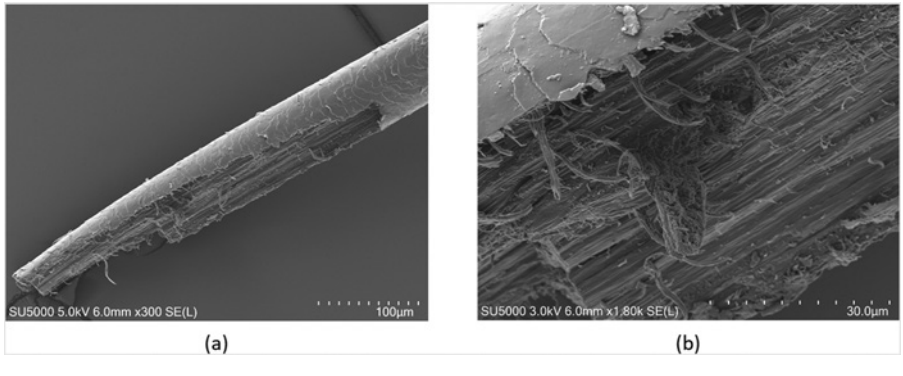

Figure 16. FESEM micrographs of a step fracture in Caucasian hair at (A) low and (B) high magnifications.

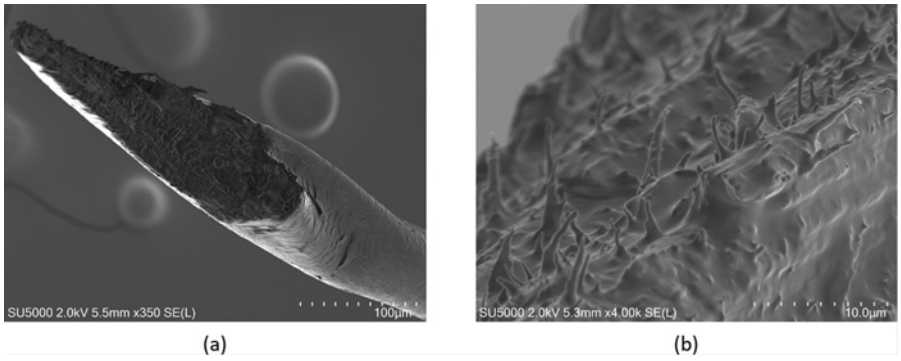

Figure 17. FESEM micrographs of (A) an angle or slanted step fracture in African hair and (B) a close-up view of a fracture region.

hair has unique fracture behavior, possibly due to its higher lipid levels or other biological components not yet identified.

A typical fracture pattern observed in Caucasian hair is found in Figure 16A. Such a pattern can be classified as a step fracture. In this case, there are two steps within the step fracture. In some cases, we observed that this type of fracture can be a relatively uniform cut along the axis of the fiber (containing only one step). Figure 16B contains a closer view of the step fracture in Figure 16A. The overall characteristics of the extended, broken fibrils were observed in all the Caucasian hair samples we examined.

Figure 17A presents an example of an angle or slanted step fracture pattern in tightly curled African hair. It is immediately apparent—as compared to Caucasian hair—that there are shorter broken fibrils in tightly curled African hair. A close-up view of one of the fracture zones (Figure 17B) reveals shorter extended fibrils that appear to be heavily coated with a nonfibrillar substance, perhaps lipids.

CONCLUSION

In this work, we investigated the physicochemical properties of textured hair, specifically African hair with *CI* values of 0.45 ± 0.08 and 0.63 ± 0.13. General morphological and fine structural details of textured hair were compared with Caucasian hair, and the unique geometrical aspects of the fibers were qualitatively described. The lipid distribution levels were determined by examining cross-sections of hair fibers where it was found that African hair had greater quantities of lipids than Caucasian hair. These data were corroborated by DVS data that demonstrated that the water uptake of African hair is less than that found in Caucasian hair. The morphology and fine structure of hair were further examined by preparing cross-sections of hair. African hair did not contain a well-developed medulla, such as that found in Asian or Caucasian hair. More than likely, this is due to the slower growth rate of African hair, which allows the cortex to become more fully developed. Tensile strength studies yielded break stress data in agreement with previous studies in the literature. We also examined the fracture patterns of fibers subjected to tensile testing with FESEM. African hair experiences various types of fracture patterns when subjected to mechanical tensile strain. African hair is unique from Caucasian hair in terms of the dimensions of the fibril remnants that are present after fiber fracture.

ACKNOWLEDGMENTS

The authors would like to express their gratitude to the R&D management team at Ashland LLC for their support of this project.

REFERENCES

(1) R. de la Mettrie, D. Saint-Léger, G. Loussouarn, A.-L. Garcel, C. Porter, and A. Langaney, Shape variability and classification of human hair: a worldwide approach, *Hum. Biol.*, **79**(3), 265–281 (2007).

(2) N. P. Khumalo, P. T. Doe, R. P. Dawber, and D. J. Ferguson, What is normal black African hair? A light and scanning electron-microscopic study, *J. Am. Acad. Dermatol.*, **43**(5 Pt. 1), 814–820 (2000).

(3) A. McMichael, Ethnic hair update: past and present, *J. Am. Acad. Dermatol.*, **48**(Suppl. 6), S127–S133 (2003).

(4) C. E. Porter, F. Dixon, C. C. Khine, B. Pistorio, H. Bryant, and R. de la Mettrie, The behavior of hair from different countries, *J. Cosmet. Sci.*, **60**(2), 97–109 (2009).

(5) T. Takahashi, Unique hair properties that emerge from combinations of multiple races, *Cosmetics*, **6**(2), 36 (2019).

(6) L. J. Wolfram, Human hair: a unique physicochemical composite, *J. Am. Acad. Dermatol.*, **48**(6 Suppl.), S106–S114 (2003).

(7) Y. Kamath, S. Hornby, and H.-D. Weigmann, Mechanical and fractographic behavior of Negroid hair, *J. Soc. Cosmet. Chem.*, **35**(1), 21–43 (1984).

(8) L. Coderch, M. A. Oliver, V. Carrer, A. M. Manich, and M. Martí, External lipid function in ethnic hairs, *J. Cosmet. Dermatol.*, **18**(6), 1912–1920 (2019).

(9) C. F. Cruz, M. M. Fernandes, A. C. Gomes, L. Coderch, M. Martí, S. Méndez, L. Gales, N. G. Azoia, U. Shimanovich, and A. Cavaco-Paulo, Keratins and lipids in ethnic hair, *Int. J. Cosmet. Sci.*, **35**(3), 244–249 (2013).

(10) M. Martí, C. Barba, A. M. Manich, L. Rubio, C. Alonso, and L. Coderch, The influence of hair lipids in ethnic hair properties, *Int. J. Cosmet. Sci.*, **38**(1), 77–84 (2016).

(11) B. A. Benard, Hair shape of curly hair, *J. Am. Acad. Dermatol.*, **48**(Suppl. 6), S120–S126 (2003).

(12) W. G. Bryson, D. P. Harland, J. P. Caldwell, J. A. Vernon, R. J. Walls, J. L. Woods, S. Nagase, T. Itou, and K. Koike, Cortical cell types and intermediate filament arrangements correlate with fiber curvature in Japanese human hair, *J. Struct. Biol.*, **166**(1), 46–58 (2009).

(13) D. P. Harland, J. A. Vernon, J. L. Woods, S. Nagase, T. Itou, K. Koike, D. A. Scobie, A. J. Grosvenor, J. M. Dyer, and S. Clerens, Intrinsic curvature in wool fibres is determined by the relative length of orthocortical and paracortical cells, *J. Exp. Biol.*, **221**(6), jeb172312 (2018).

(14) Y. Kajiura, S. Watanabe, T. Itou, K. Nakamura, A. Iida, K. Inoue, N. Yagi, Y. Shinohara, and Y. Amemiya, Structural analysis of human hair single fibres by scanning microbeam SAXS, *J. Struct. Biol.*, **155**(3), 438–444 (2006).

(15) S. Nagase, T. Shinozaki, M. Tsuchiya, H. Tsujimura, Y. Masukawa, N. Satoh, T. Itou, and K. Koike, Characteristic microstructure of curved human hair, *Int. J. Cosmet. Sci.*, **32**(4), 317 (2010).

(16) S. Nagase, M. Tsuchiya, T. Matsui, S. Shibuichi, H. Tsujimura, Y. Masukawa, N. Satoh, T. Itou, K. Koike, and K. Tsujii, Characterization of curved hair of Japanese women with reference to internal structures and amino acid composition, *J. Cosmet. Sci.*, **59**(4), 317–332 (2008).

(17) J. N. Nissimov and A. B. Das Chaudhuri, Hair curvature: a natural dialectic and review, *Biol. Rev. Camb. Philos. Soc.*, **89**(3), 723–766 (2014).

(18) S. Thibaut, P. Barbarat, F. Leroy, and B. A. Bernard, Human hair keratin network and curvature, *Int. J. Dermatol.*, **46**(Suppl. 1), 7–10 (2007).

(19) M. Wade, I. Tucker, P. Cunningham, R. Skinner, F. Bell, T. Lyons, K. Patten, L. Gonzalez, and T. Wess, Investigating the origins of nanostructural variations in differential ethnic hair types using X-ray scattering techniques, *Int. J. Cosmet. Sci.*, **35**(5), 430–441 (2013).

(20) B. Xu and X. Chen, The role of mechanical stress on the formation of a curly pattern of human hair, *J. Mech. Behav. Biomed. Mater.*, 4(2), 212–221 (2011).

(21) G. E. Westgate, R. S. Ginger, and M. R. Green, The biology and genetics of curly hair, *Exp. Dermatol.*, **26**(6), 483–490 (2017).

(22) K. Keis, K. R. Ramaprasad, and Y. K. Kamath, Studies of light scattering from ethnic hair fibers, *J. Cosmet. Sci.*, **55**(1), 49–63 (2004).

(23) R. McMullen and J. Jachowicz, Optical properties of hair—detailed examination of specular reflection patterns in various hair types, *J. Cosmet. Sci.*, **55**(1), 29–47 (2004).

(24) J. Menkart, L. Wolfram, and I. Mao, Caucasian hair, negro hair, and wool: similarities and differences, *J. Soc. Cosmet. Chem.*, **17**(13), 769–787 (1966).

(25) C. Nappe and M. Kermici, Electrophoretic analysis of alkylated proteins of human hair from various ethnic groups, *J. Soc. Cosmet. Chem.*, **40**(2), 91–99 (1989).

(26) H. A. Adeola, N. P. Khumalo, A. T. Arowolo, and N. Mehlala, No difference in the proteome of racially and geometrically classified scalp hair sample from a South African cohort: preliminary findings, *J. Proteomics*, **226**, 103892 (2020).

(27) K. Adhikari, T. Fontanil, S. Cal, J. Mendoza-Revilla, M. Fuentes-Guajardo, J.-C. Chacón-Duque, F. Al-Saadi, J. A. Johansson, M. Quinto-Sanchez, V. Acuña-Alonzo, C. Jaramillo, W. Arias, R. Barquera Lozano, G. Macín Pérez, J. Gómez-Valdés, H. Villamil-Ramírez, T. Hunemeier, V. Ramallo, C. Silva de Cerqueira, M. Hurtado, V. Villegas, V. Granja, C. Gallo, G. Poletti, L. Schuler-Faccini, F. M. Salzano, M.-C. Bortolini, S. Canizales-Quinteros, F. Rothhammer, G. Bedoya, R. Gonzalez-José, D. Headon, C. López-Otín, D. J. Tobin, D. Balding, and A. Ruiz-Linares, A genome-wide association scan in admixed Latin Americans identifies loci influencing facial and scalp hair features, *Nat. Commun.*, **7**, 10815 (2016).

(28) J. D. dos Santos, H. G. M. Edwards, and L. F. C. de Oliveira, Raman spectroscopy and electronic microscopy structural studies of Caucasian and Afro human hair, *Heliyon*, **5**(5), e01582 (2019).

(29) J. H. Ji, T.-S. Park, H.-J. Lee, Y.-D. Kim, L.-Q. Pi, X.-H. Jin, and W.-S. Lee, The ethnic differences of the damage of hair and integral hair lipid after ultraviolet radiation, *Ann. Dermatol.*, **25**(1), 54–60 (2013).

(30) Y. Kamath, S. Hornby, and H.-D. Weigmann, Effect of chemical and humectant treatments on the mechanical and fractographic behavior of Negroid hair. *J. Soc. Cosmet. Chem.*, **36**(1), 39–52 (1985).

(31) T. Mamabolo, N. M. Agyei, and B. Summers, Cosmetic and amino acid analysis of the effects of lye and no-lye relaxer treatment on adult black female South African hair, *J. Cosmet. Sci.*, **64**(4), 287–296 (2013).

(32) L. J. Wolfram, On straightening and relaxing of African hair, *J. Cosmet. Sci.*, **66**(3), 207–210 (2015).

(33) L. Kreplak, F. Briki, Y. Duvault, J. Doucet, C. Merigoux, F. Leroy, J. L. Lévêque, L. Miller, G. L. Carr, G. P. Williams, and P. Dumas, Profiling lipids across Caucasian and Afro-American hair transverse cuts, using synchrotron infrared microspectrometry, *Int. J. Cosmet. Sci.*, **23**(6), 369–374 (2001).

(34) R. L. McMullen, D. Laura, S. Chen, D. Koelmel, G. Zhang, and T. Gillece, Determination of physicochemical properties of delipidized hair, *J. Cosmet. Sci.*, **64**(5), 355–370 (2013).

(35) Y. K. Kamath, Quantification of human hair moisturization with cosmetic products by dynamic vapor sorption, *J. Cosmet. Sci.*, **71**(5), 303–320 (2020).

(36) F.-J. Wortmann, A. Hullmann, and C. Popescu, Water management of human hair, *Int. J. Cosmet. Sci.*, **30**(5), 388–389 (2008).

(37) S. Chahal, N. Challoner, and R. Jones, Moisture regulation of hair by cosmetic proteins as demonstrated by dynamic vapour sorption—a novel efficacy testing technique, *IFSCC Mag.*, **3**(2), 19–25 (2000).

(38) T. Evans, "Adsorption properties of hair," in *Practical Modern Hair Science*. T. Evans and R. Wickett. Eds. (Allured Publishing, Carol Stream, IL, 2012), pp. 333–365.

(39) C. Barba, M. Martí, J. Carilla, A. M. Manich, and L. Coderch, Moisture sorption/desorption of protein fibres, *Thermochim. Acta*, **552**, 70–76 (2013).

(40) A. Franbourg, P. Hallegot, F. Baltenneck, C. Toutain, and F. Leroy, Current research on ethnic hair, *J. Am. Acad. Dermatol.*, **48**(6 Suppl.), S115–S119 (2003).

(41) M. Steggerda, Cross sections of human hair from four racial groups, *J. Hered.*, **31**(11), 474–476 (1940).